

## Reversible Enolization of $\beta$ -Amino Carboxamides by Lithium Hexamethyldisilazide

Anne J. McNeil and David B. Collum\*

Contribution from the Department of Chemistry and Chemical Biology, Baker Laboratory, Cornell University, Ithaca, New York 14853-1301

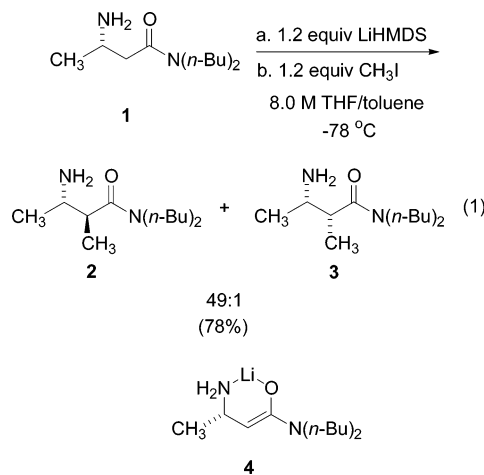
Received October 28, 2004; E-mail: dbc6@cornell.edu

**Abstract:** The enolization of  $\beta$ -amino carboxamides by lithium hexamethyldisilazide (LiHMDS) in THF/toluene and subsequent diastereoselective alkylation with  $\text{CH}_3\text{I}$  are reported. In situ IR spectroscopic studies reveal that  $\beta$ -amino carboxamides coordinate to LiHMDS at  $-78^\circ\text{C}$  before enolization. Comparison with structurally similar carboxamides suggests that the  $\beta$ -amino group promotes the enolization. IR spectroscopic studies also show that the enolization is reversible. Efficient trapping of the enolate by  $\text{CH}_3\text{I}$  affords full conversion to products.  $^6\text{Li}$  and  $^{15}\text{N}$  NMR spectroscopic studies reveal that lithium enolate–LiHMDS mixed dimers and trimers as well as a homoaggregated enolate are formed during the reaction. At ambient temperature, racemization of the  $\beta$ -position through a putative reversible Michael addition was observed.

### Introduction

As an adjunct to investigations of the enolization and alkylation of  $\beta$ -amino esters,<sup>1</sup> we had occasion to study the enolization and alkylation of  $\beta$ -amino carboxamides (eq 1).<sup>2</sup> The protocol, using an unprotected amino group,<sup>3–5</sup> is synthetically interesting given the biochemical and pharmaceutical importance of  $\beta$ -amino amides<sup>6</sup> and  $\beta$ -amino acids.<sup>7</sup> Furthermore, the reversible enolization suggests an underlying complexity that piqued our interest. The  $\beta$ -amino group may also be important because enolizations of carboxamides generally require bases stronger than lithium hexamethyldisilazide (LiHMDS).<sup>8</sup>

We show herein that the LiHMDS-mediated enolization of **1**<sup>9</sup> affords an equilibrium mixture of **1** and enolate **4**. The high yields of alkylated product derive from a relatively slow enolization followed by an efficient trapping of enolate **4** with  $\text{CH}_3\text{I}$ . We also show, however, that this seemingly simple transformation belies a complex ensemble of lithium enolate mixed aggregates. Moreover, an NMR spectroscopic technique in conjunction with a Job plot suggests that the homoaggregate of the enolate is hexameric.



- (1) (a) McNeil, A. J.; Toombes, G. E. S.; Chandramouli, S. V.; Vanasse, B. J.; Ayers, T. A.; O'Brien, M. K.; Lobkovsky, E.; Gruner, S. M.; Marohn, J. A.; Collum, D. B. *J. Am. Chem. Soc.* **2004**, *126*, 5938–5939. (b) McNeil, A. J.; Toombes, G. E. S.; Gruner, S. M.; Lobkovsky, E.; Collum, D. B.; Chandramouli, S. V.; Vanasse, B. J.; Ayers, T. A. *J. Am. Chem. Soc.* **2004**, *126*, 16559–16568.
- (2) An X-ray crystal structure of the *N*-Boc derivative of **2** was used to assign the stereochemistry for the major product of the alkylation.  $^1\text{H}$  NMR spectra ( $d_6$ -THF) recorded on the *N*-Boc derivatives of **2** and **3** gave coupling constants for the  $\alpha$ -H of 3.5 and 8.8 Hz, respectively (Supporting Information).
- (3) Chandramouli, S. V.; O'Brien, M. K.; Pownner, T. H. WO Patent, 0040547, 2000.
- (4) A similar enolization and alkylation of an unprotected  $\beta$ -alanine pseudoephedrine carboxamide with LiHMDS/MeI/LiCl at  $0^\circ\text{C}$  in THF has been reported: Nagula, G.; Huber, V. J.; Lum, C.; Goodman, B. A. *Org. Lett.* **2000**, *2*, 3527–3529.
- (5) Enolates derived from unprotected  $\alpha$ -amino amides have been alkylated: (a) Myers, A. G.; Schnider, P.; Kwon, S.; Kung, D. W. *J. Org. Chem.* **1999**, *64*, 3322–3327. (b) Myers, A. G.; Gleason, J. L.; Yoon, T.; Kung, D. W. *J. Am. Chem. Soc.* **1997**, *119*, 656–673. (c) Roy, R. S.; Imperiali, B. *Tetrahedron Lett.* **1996**, *37*, 2129–2132. (d) Myers, A. G.; Yoon, T.; Gleason, J. L. *Tetrahedron Lett.* **1995**, *36*, 4555–4558. (e) Myers, A. G.; Gleason, J. L.; Yoon, T. *J. Am. Chem. Soc.* **1995**, *117*, 8488–8489.
- (6) For related alkylations of *N*-protected  $\beta$ -amino carboxamide enolates, see: (a) Gutiérrez-García, V. M.; Reyes-Rangel, G.; Muñoz-Muñoz, O.; Juaristi, E. *Helv. Chim. Acta* **2002**, *85*, 4189–4199. (b) Gutiérrez-García, V. M.; López-Ruiz, H.; Reyes-Rangel, G.; Juaristi, E. *Tetrahedron* **2001**, *57*, 6487–6496. (c) Ponsinet, R.; Chassaing, G.; Vaissermann, J.; Lavielle, S. *Eur. J. Org. Chem.* **2000**, 83–90. (d) Davies, S. G.; Edwards, A. J.; Walters, I. A. S. *Recl. Trav. Chim. Pays-Bas* **1995**, *114*, 175–183. (e) Kurihara, T.; Terada, T.; Satoda, S.; Yoneda, R. *Chem. Pharm. Bull.* **1986**, *34*, 2786–2798. (f) McGarvey, G. J.; Williams, J. M.; Hiner, R. N.; Matsubara, Y.; Oh, T. *J. Am. Chem. Soc.* **1986**, *108*, 4943–4952. (g) Yoneda, R.; Terada, T.; Satoda, S.; Kurihara, T. *Heterocycles* **1985**, *23*, 2243–2246.

- (7) (a) *Enantioselective Synthesis of  $\beta$ -Amino Acids*; Juaristi, E., Ed.; Wiley-VCH: New York, 1997. (b) Sewald, N. *Angew. Chem., Int. Ed.* **2003**, *42*, 5794–5795. (c) Ma, J.-A. *Angew. Chem., Int. Ed.* **2003**, *42*, 4290–4299. (d) Liu, M.; Sibi, M. P. *Tetrahedron* **2002**, *58*, 7991–8035. (e) Abele, S.; Seebach, D. *Eur. J. Org. Chem.* **2000**, 1–15. (f) Cardillo, G.; Tomasini, C. *Chem. Soc. Rev.* **1996**, 117–128. (g) Cole, D. C. *Tetrahedron* **1994**, *32*, 9517–9582. (h) Juaristi, E.; Quintana, D.; Escalante, J. *Aldrichimica Acta* **1994**, *27*, 3–11.
- (8) For example, see: Coumbarides, G. S.; Eames, J.; Ghilgaber, S. J. *Labelled Compd. Radiopharm.* **2003**, *46*, 1033–1053.
- (9) The *N,N*-di-*n*-butyl moiety offers superior solubility in THF/toluene solutions at  $-78^\circ\text{C}$  when compared to structurally related  $\beta$ -amino carboxamide enolates.

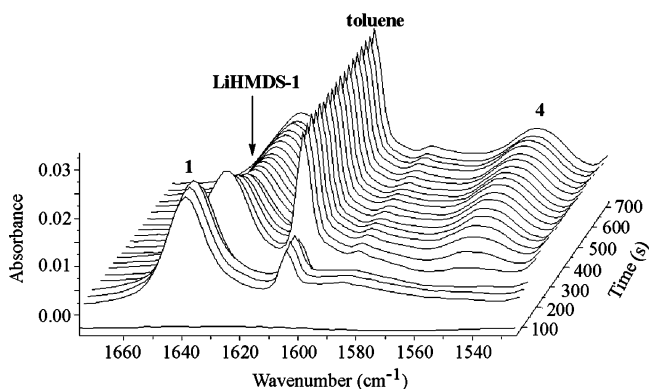


**Figure 1.** In situ IR spectra showing the enolization of **1** (0.01 M) with LiHMDS (0.02 M) in 10.2 M THF/toluene at  $-78\text{ }^{\circ}\text{C}$ .

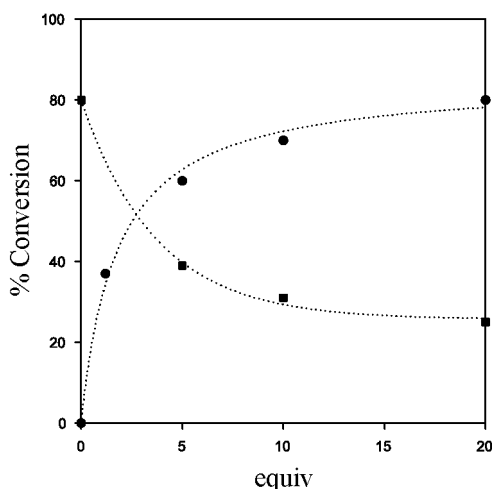


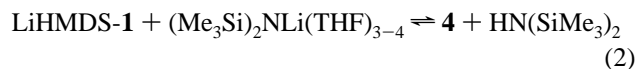
**Figure 2.** Plot of the percent conversion for the enolization of **1** (0.01 M) with LiHMDS in 8.0 M THF/toluene at  $-78\text{ }^{\circ}\text{C}$  vs the equivalents of added LiHMDS (●) and HMDS (■).

## Results and Discussion

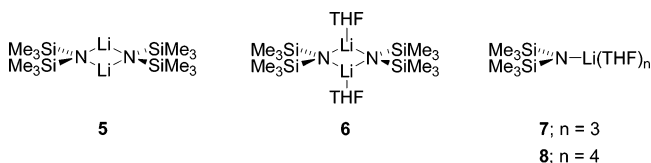
**Reversible Enolization.** Treatment of **1** with  $>1.0$  equiv of LiHMDS in 0.6–12.3 M THF/toluene at  $-78\text{ }^{\circ}\text{C}$  causes a  $10\text{ cm}^{-1}$  shift in the carbonyl stretch of **1** (from  $1640$  to  $1630\text{ cm}^{-1}$ ), indicating that **1** quantitatively coordinates to LiHMDS (Figure 1). Subsequent enolization affords **4** ( $1550\text{ cm}^{-1}$ ) and significant concentrations of unreacted **1** still coordinated to lithium ( $1630\text{ cm}^{-1}$ ). In short, the reaction stalls.

It is quite common for intervening mixed aggregates to decelerate organolithium reactions because of their markedly lower reactivity,<sup>10,11</sup> and, indeed, mixed aggregates derived from LiHMDS and **4** are observed (vide infra). In this case, however, the incomplete conversion is due to an equilibration described generically by eq 2 and shown in Figure 2. For example, addition of 1.2 equiv of LiHMDS (0.012 M) in 8.0 M THF/toluene affords enolate **4** at 37% conversion, whereas addition of 20 equiv of LiHMDS (0.20 M) increases the conversion to 80%. The reversibility of the enolization was confirmed when added hexamethyldisilazane (HMDS) caused an enolization at 80% conversion to revert to 25% conversion. Despite the highly

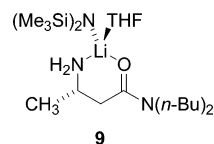
[THF]-dependent structures of both LiHMDS<sup>12</sup> and lithium enolate–LiHMDS mixed aggregates (vide infra), the percent conversion is invariant over a 10-fold range of THF concentrations (1.0–10 M).<sup>13</sup>



**Structural Studies: General.** We used a combination of  $^6\text{Li}$  and  $^{15}\text{N}$  NMR spectroscopic studies to investigate the LiHMDS-**1** complexes and the lithium enolate aggregates formed during the enolization. Previous work revealed that LiHMDS exists as dimer **5** in neat toluene;<sup>14</sup> disolvated dimer **6** in toluene containing low concentrations of THF; and tri- and tetrasolvated monomers **7** and **8** at high concentrations of THF.<sup>12</sup>



**Substrate–LiHMDS Complexation.** IR spectroscopic studies show that the carboxamide moiety of **1** readily coordinates to LiHMDS under conditions in which LiHMDS is predominantly monomeric.<sup>12</sup>  $^6\text{Li}$  NMR spectra recorded on mixtures of carboxamide **1** and [ $^6\text{Li}$ ,  $^{15}\text{N}$ ]LiHMDS in  $>2.0$  M THF/toluene afford the  $^6\text{Li}$  resonances corresponding to enolate **4**, LiHMDS dimer **6**, and LiHMDS monomer. The spectra show a larger LiHMDS monomer/dimer ratio, and the monomer signal is downfield compared to carboxamide-free THF solutions, implicating complex **9**, consistent with previous studies of LiHMDS solvated by bidentate ligands.<sup>15</sup>



At lower THF concentrations—conditions that promote the LiHMDS dimer—IR spectroscopy shows clear evidence of the  $\beta$ -amino carboxamide binding to lithium ( $1630\text{ cm}^{-1}$ ), yet the  $^6\text{Li}$  NMR spectra show no changes that could be construed as evidence of coordination or even formation of a new species. To ascertain whether the NMR spectral result was inherent to the coordination chemistry of the carboxamide moiety, we briefly investigated the ligating properties of a structurally analogous carboxamide and found that carboxamide binding to the LiHMDS dimer in neat toluene and low THF concentrations

(10) For leading references to mixed aggregation effects on organolithium reactions, see: (a) Pratt, L. M.; Streitwieser, A. *J. Org. Chem.* **2003**, *68*, 2830–2838. (b) Seebach, D. *Angew. Chem., Int. Ed. Engl.* **1988**, *27*, 1624–1654.  
 (11) For leading references to decelerations owing to formation of lithium amide mixed aggregates, see: Sun, X.; Collum, D. B. *J. Am. Chem. Soc.* **2000**, *122*, 2459–2463.

(12) For leading references, see: (a) Lucht, B. L.; Collum, D. B. *Acc. Chem. Res.* **1999**, *32*, 1035–1042. (b) Lucht, B. L.; Collum, D. B. *J. Am. Chem. Soc.* **1995**, *117*, 9863–9874. (c) Lucht, B. L.; Collum, D. B. *J. Am. Chem. Soc.* **1994**, *116*, 6009–6010.  
 (13) At less than 1.0 equiv of THF per lithium, however, we observed a significant decrease in the extent of enolization with 20 equiv of LiHMDS. Conversely, we observed an inverse [THF]-dependence on the extent of enolization when excess HMDS was present.  
 (14) LiHMDS dimer **5** is stabilized in toluene relative to a higher oligomer owing to a hydrocarbon–lithium interaction: Lucht, B. L.; Collum, D. B. *J. Am. Chem. Soc.* **1996**, *118*, 2217–2225.  
 (15) Lucht, B. L.; Bernstein, M. P.; Remenar, J. F.; Collum, D. B. *J. Am. Chem. Soc.* **1996**, *118*, 10707–10718.

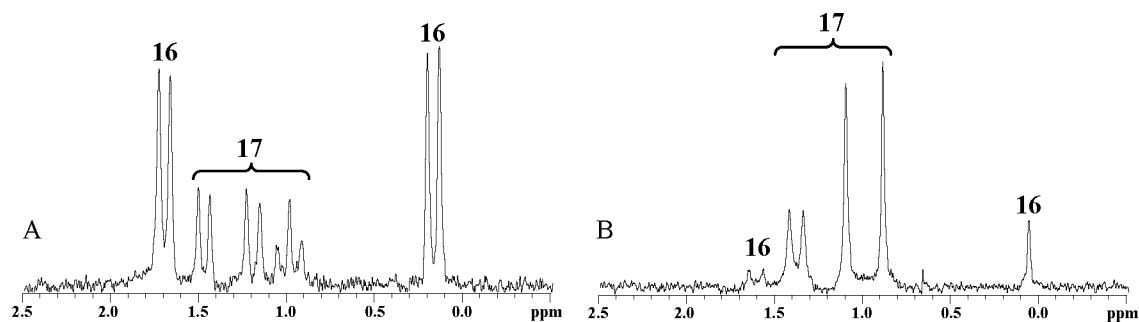


**Figure 3.**  $^6\text{Li}$  NMR spectra recorded in neat toluene at  $-75\text{ }^\circ\text{C}$ . (A)  $[\text{}^6\text{Li}, \text{}^{15}\text{N}]\text{LiHMDS}$  (0.08 M), **1** (0.023 M). (B)  $[\text{}^6\text{Li}]\text{LiHMDS}$  (0.08 M),  $[\text{}^{15}\text{N}]\text{1}$  (0.023 M).<sup>23</sup>

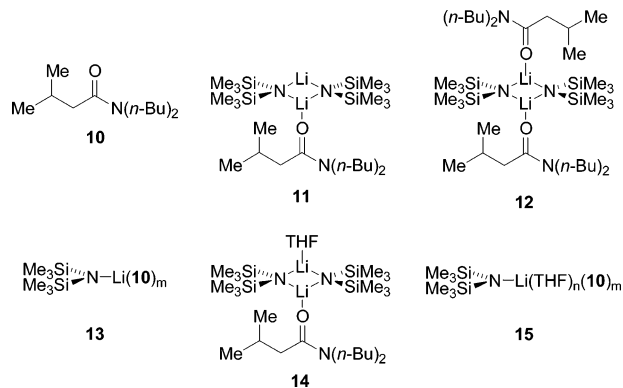
**Table 1.**  $^6\text{Li}$  and  $^{15}\text{N}$  NMR Spectral Data of LiHMDS/4 Aggregates<sup>a</sup>

| compd      | $^6\text{Li}$ $\delta$ (mult, $J_{\text{LN}}$ ) <sup>b</sup> | $^6\text{Li}$ (mult, $J_{\text{LN}}$ ) <sup>c</sup> | $^{15}\text{N}$ $\delta$ (mult, $J_{\text{LN}}$ ) <sup>b</sup> | $^{15}\text{N}$ $\delta$ (mult, $J_{\text{LN}}$ ) <sup>c</sup> |
|------------|--|---|--|--|
| <b>5</b>   | 0.35 (t, 3.5)  | —   | 43.0 (q, 3.7)  | —  |
| <b>6</b>   | 1.0 (t, 3.4)   | —   | 38.5 (q, 3.4)  | —  |
| <b>7/8</b> | 0.01 (d, 5.1)  | —   | 41.9 (t, 4.9)  | —  |
| <b>9</b>   | 0.14 (d, 4.8)  | <i>d</i>  | 42.0 (t, 5.0)  | —  |
| <b>16</b>  | 0.19 (d, 4.0)  | —   | 40.7 (q, 3.9)  | 49.9 (t, 4.3)  |
|            | 1.72 (d, 3.8)  | (d, 4.3)  | —  | —  |
| <b>17</b>  | 1.01 (t, 4.5)  | —   | 42.9 (q, 4.1)  | 46.7 (t, 4.0)  |
|            | 1.22 (d, 4.4)  | —   | 45.4 (q, 4.3)  | —  |
|            | 1.50 (d, 3.9)  | (d, 4.5)  | —  | —  |
| <b>19</b>  | 0.96   | (d, 3.9)  | —  | 43.9 <sup>e,f</sup>  |
| <b>20</b>  | 0.61 (d, 3.1)  | <i>d</i>  | 43.5 <sup>e</sup>  | 51.7 <sup>e</sup>  |

<sup>a</sup> Spectra were recorded on 0.08 M Li solutions at various THF concentrations with toluene at  $-75\text{ }^\circ\text{C}$ . Multiplicities are denoted as follows: d = doublet, t = triplet, q = quintet. The chemical shifts are reported relative to 0.3 M  $^6\text{LiCl}/\text{MeOH}$  at  $-90\text{ }^\circ\text{C}$  (0.0 ppm) and neat  $\text{Me}_2\text{NEt}$  (25.7 ppm). All  $J$  values are reported in hertz. <sup>b</sup> Spectra were recorded with  $[\text{}^6\text{Li}, \text{}^{15}\text{N}]\text{LiHMDS}$  and  $[\text{}^{14}\text{N}]\text{1}$ . <sup>c</sup> Spectra were recorded with  $[\text{}^6\text{Li}]\text{LiHMDS}$  and  $[\text{}^{15}\text{N}]\text{1}$ . <sup>d</sup> Coupling was poorly resolved in the  $^6\text{Li}$  NMR spectra. <sup>e</sup> Coupling was poorly resolved in the  $^{15}\text{N}$  NMR spectra. <sup>f</sup> There were two unassigned resonances (42.8, 44.9).

is readily observed by  $^6\text{Li}$  NMR spectroscopy.<sup>16,17</sup> We also examined the binding of *sec*-BuNH<sub>2</sub> to LiHMDS in neat toluene and low THF concentrations and found that it too binds readily to the LiHMDS dimer with the consequent formation of new resonances.<sup>18</sup> We are unsure as to why carboxamide **1** does not elicit similar spectral changes but suspect it may be forming extended structures as noted previously for bidentate ligands.<sup>15</sup>

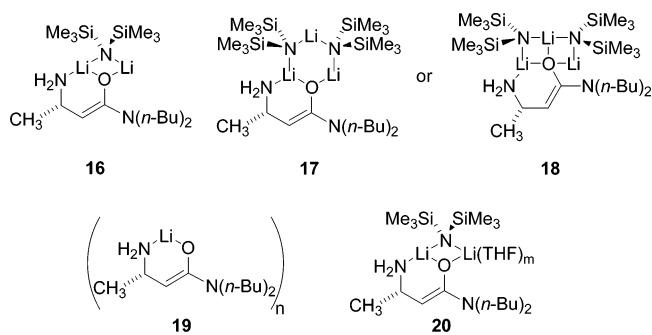
(16) Serial additions of carboxamide **10** to LiHMDS in toluene afford sequentially (1) mono- and disolvated dimers **11** and **12** (respectively) at  $<1.0$  equiv of **10**, and (2) monomer **13** with excess **10**. Analogous serial additions in 2.0 M THF/toluene afford (sequentially) **14**, **12**, and **15**. It is notable that **10** does not enolize even with warming to ambient temperature. Furthermore, IR spectroscopy shows that the C=O moiety of  $\beta$ -amino carboxamide **1** binds quantitatively in THF, whereas isostructural carboxamide **10** does not, indicating that chelation of lithium by the  $\beta$ -NH<sub>2</sub> is important (Supporting Information).



(17) Carboxamide **10** was prepared using methyl isovalerate and  $\text{Et}_3\text{Al}/\text{Bu}_2\text{NH}$ . Patterson, J. W. *J. Org. Chem.* **1995**, *60*, 4542–4548.

(18) Analogous  $^6\text{Li}$  and  $^{15}\text{N}$  NMR spectroscopic studies on mixtures of  $[\text{}^6\text{Li}, \text{}^{15}\text{N}]\text{LiHMDS}$  and *sec*-BuNH<sub>2</sub> are archived in Supporting Information. Also, see ref 14.

**Structures of Lithium Enolate–LiHMDS Mixed Aggregates.** We initiated studies of mixed aggregation based on enolizations using neat toluene. Figure 3 shows that the enolization of **1** in toluene mediated by excess LiHMDS affords mixed dimer **16** and mixed trimer **17** (or isomeric ladder **18**).  $^6\text{Li}$ – $^{15}\text{N}$  couplings from both  $[\text{}^6\text{Li}, \text{}^{15}\text{N}]\text{LiHMDS}$  and  $[\text{}^{15}\text{N}]\text{1}$  (Table 1) are consistent with the proposed structures.<sup>19</sup> Related lithium enolate–lithium amide mixed aggregates have been observed both spectroscopically<sup>20</sup> and crystallographically.<sup>21,22</sup>



In general, cyclic trimers and higher oligomers of lithium amides are converted to lower aggregates by adding coordinating

(19) For calculations of  $^6\text{Li}$ – $^{15}\text{N}$  coupling constants, see: (a) Parisel, O.; Fressigné, C.; Maddaluno, J.; Giessner-Prettre, C. *J. Org. Chem.* **2003**, *68*, 1290–1294. (b) Koizumi, T.; Morihashi, K.; Kikuchi, O. *Bull. Chem. Soc. Jpn.* **1996**, *69*, 305–309.

(20) For spectroscopic characterization of lithium enolate–lithium amide mixed aggregates in solution, see: (a) Kim, Y.-J.; Streitwieser, A. *Org. Lett.* **2002**, *4*, 573–575. (b) Romesberg, F. E.; Collum, D. B. *J. Am. Chem. Soc.* **1994**, *116*, 9198–9202. (c) Hall, P. L.; Gilchrist, J. H.; Harrison, A. T.; Fuller, D. J.; Collum, D. B. *J. Am. Chem. Soc.* **1991**, *113*, 9575–9585. Also, see refs 1 and 11.

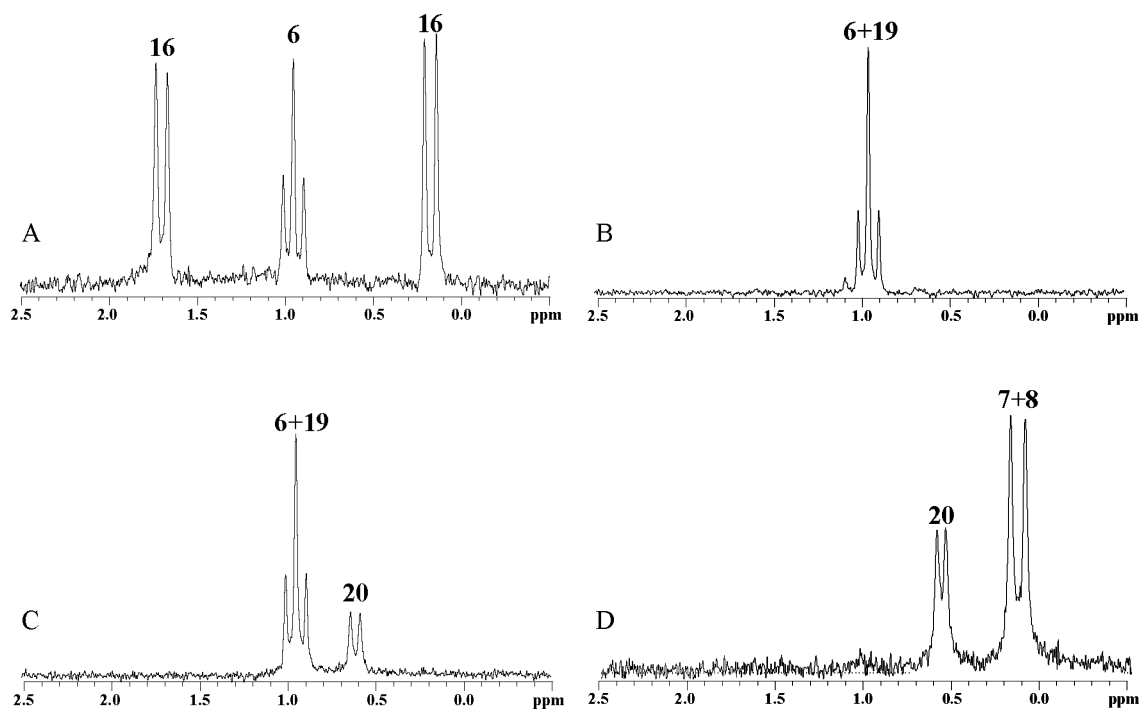


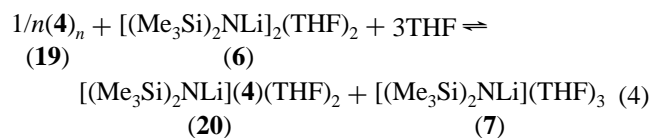
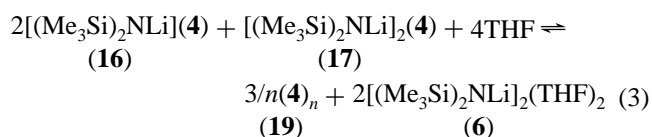
**Figure 4.**  $^6\text{Li}$  NMR spectra recorded on  $[\text{}^6\text{Li},\text{}^{15}\text{N}]\text{LiHMDS}$  (0.08 M) and **1** (0.023 M) in various THF concentrations with toluene at  $-75\text{ }^\circ\text{C}$ . (A) 0.01 M. (B) 0.06 M. (C) 0.5 M. (D) 8.0 M.

ligands.<sup>24</sup> Serial solvation of the LiHMDS-**4** dimer/trimer mixture, however, displays more complicated behavior. For example, addition of fractional equivalents of THF (<0.2 equiv/lithium) to mixed dimer **16** and mixed trimer **17** causes trimer **17** to be replaced by enolate oligomer **19** and solvated LiHMDS dimer **6**. Further addition of THF (0.5–1.0 equiv/lithium) affords LiHMDS dimer **6** and enolate **19** to the exclusion of mixed dimer **16** (Figure 4B). Although the lithium enolate could be readily detected by IR spectroscopy, a perfect superposition of the  $^6\text{Li}$  resonances of **6** and **19** made it particularly challenging to detect **19** using  $^6\text{Li}$  NMR spectroscopy. The superposition was noted by (1) the anomalously high integration of the center triplet of **6** in  $[\text{}^6\text{Li},\text{}^{15}\text{N}]\text{LiHMDS}/\mathbf{4}$  mixtures, and (2) the doublet flanking the signal of **6** in analogous solutions prepared from  $[\text{}^6\text{Li}]\text{LiHMDS}$  and  $[\text{}^{15}\text{N}]\mathbf{1}$  that was confirmed by  $^{15}\text{N}$  decoupling. We found that the homoaggregated enolate could be generated as the sole observable form of the enolate

by using 1.0 equiv of  $[\text{}^6\text{Li}]\text{LiHMDS}$  and 0.8 equiv of THF, allowing us to characterize **19** as described in the next section.

Further addition of THF (>1.0 equiv/lithium) caused the mixed dimer to *reappear* in a solvated form (**20**; Figure 4C). An analogous mixed dimer derived from  $\beta$ -amino ester enolates was previously observed.<sup>1</sup> Mixed dimer **20** displays coupling constants consistent with a cyclic dimer motif<sup>19</sup> and appears as a single  $^6\text{Li}$  resonance at  $-75\text{ }^\circ\text{C}$  that resolves into two broad resonances on cooling to  $-115\text{ }^\circ\text{C}$  (Supporting Information). At high THF concentrations, the lithium enolate exists exclusively as mixed dimer **20**, and the excess LiHMDS is converted to monomers **7/8** (Figure 4D).

The disappearance of mixed dimer **16** at low concentrations of THF and the reappearance of THF-solvated mixed dimer **20** at higher THF concentrations, although odd on first inspection, may be understood through the balanced expressions described by eqs 3 and 4. Related phenomena were observed for mixtures of LiHMDS solvated by a protic diamine.<sup>25</sup>



**Structure of Enolate Homoaggregates.** We previously reported a strategy to assign the structure of homoaggregated  $\beta$ -amino ester enolates in solution using variable-temperature  $^6\text{Li}$  NMR spectroscopy.<sup>1</sup> In short, warming the sample to

- (21) For crystal structures of lithium enolate–lithium amide mixed aggregates, see: (a) Williard, P. G.; Hintze, M. J. *J. Am. Chem. Soc.* **1990**, *112*, 8602–8604. (b) Williard, P. G.; Hintze, M. J. *J. Am. Chem. Soc.* **1987**, *109*, 5539–5541. Also, see ref 10b.
- (22) Lithium enolate–lithium amide mixed aggregates have been examined computationally: (a) Pratt, L. M.; Newman, A.; Cyr, J. S.; Johnson, H.; Miles, B.; Lattier, A.; Austin, E.; Henderson, S.; Hershey, B.; Lin, M.; Balamraju, Y.; Sammonds, L.; Cheramie, J.; Karnes, J.; Hymel, E.; Woodford, B.; Carter, C. *J. Org. Chem.* **2003**, *68*, 6387–6391. (b) Henderson, K. W.; Dorigo, A. E.; Liu, Q.-Y.; Williard, P. G.; Schleyer, P. v. R.; Bernstein, P. R. *J. Am. Chem. Soc.* **1996**, *118*, 1339–1347. (c) Romesberg, F. E.; Collum, D. B. *J. Am. Chem. Soc.* **1994**, *116*, 9187–9197. Also, see ref 10a.
- (23) The relative intensity changes of **16** and **17** in Figure 3, parts A and B, result from unintentional stoichiometry differences from using different samples of  $\beta$ -amino carboxamide and LiHMDS.
- (24) (a) Gregory, K.; Schleyer, P. v. R.; Snaith, R. *Adv. Inorg. Chem.* **1991**, *37*, 47–142. (b) Barr, D.; Snaith, R.; Clegg, W.; Mulvey, R. E.; Wade, K. *J. Chem. Soc., Dalton Trans.* **1987**, 2141–2147. (c) Armstrong, D. R.; Barr, D.; Snaith, R.; Clegg, W.; Mulvey, R. E.; Wade, K.; Reed, D. *J. Chem. Soc., Dalton Trans.* **1987**, 1071–1081. (d) Armstrong, D. R.; Barr, D.; Clegg, W.; Mulvey, R. E.; Reed, D.; Snaith, R.; Wade, K. *J. Chem. Soc., Chem. Commun.* **1986**, 869–870. (e) Barr, D.; Clegg, W.; Mulvey, R. E.; Snaith, R.; Wade, K. *J. Chem. Soc., Chem. Commun.* **1986**, 295–297.

- (25) Lucht, B. L.; Collum, D. B. *J. Am. Chem. Soc.* **1996**, *118*, 3529–3530.

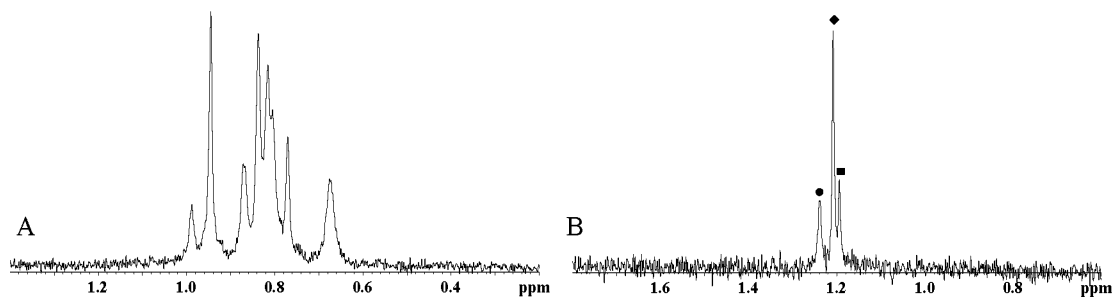


**Figure 5.**  $^6\text{Li}$  NMR spectra recorded on  $[\text{}^6\text{Li}]\text{LiHMDS}$  (0.10 M) and **1** (0.10 M,  $X_R = 0.8$ ) in 0.075 M THF/toluene at (A)  $-75^\circ\text{C}$  and (B)  $35^\circ\text{C}$ .  $\text{R}_4\text{S}_2/\text{R}_2\text{S}_4$  (●);  $\text{R}_5\text{S}_1/\text{R}_1\text{S}_5$  (◆);  $\text{R}_6/\text{S}_6$  (■).

the point at which *intra*-aggregate exchanges are fast but *inter*-aggregate exchanges remain slow produces a *single* resonance for aggregates that differ only in stereoisomerism or positional isomerism.<sup>26</sup> Aggregates that differ by subunit composition (cf., 4:2 versus 3:3 mixed hexamers) or by virtue of their aggregation numbers (cf., dimers versus tetramers) appear as separate species in the  $^6\text{Li}$  NMR spectra.

The inherent symmetry of the lithium enolate aggregates can be disrupted by using combinations of *R* and *S* antipodes to generate an ensemble of homo- and heterochiral aggregates. In the limit of rapid *intra*-aggregate exchange, dimers ( $\text{R}_1\text{S}_1$  and  $\text{R}_2/\text{S}_2$ ), tetramers ( $\text{R}_4/\text{S}_4$ ,  $\text{R}_1\text{S}_3/\text{R}_3\text{S}_1$ , and  $\text{R}_2\text{S}_2$ ), and hexamers ( $\text{R}_6/\text{S}_6$ ,  $\text{R}_1\text{S}_5/\text{R}_5\text{S}_1$ ,  $\text{R}_2\text{S}_4/\text{R}_4\text{S}_2$ , and  $\text{R}_3\text{S}_3$ ) are expected to afford two, three, and four  $^6\text{Li}$  resonances, respectively. ( $\text{R}_n\text{S}_{N-n}/\text{R}_{N-n}\text{S}_n$  and  $\text{R}_N/\text{S}_N$  refer to pairs of spectroscopically indistinguishable enantiomers.)

$^6\text{Li}$  NMR spectra recorded on *R/S* mixtures of enolate **4** contain multiple resonances at  $-75^\circ\text{C}$ , consistent with inordinate structural complexity stemming from both stereoisomerism and positional isomerism as well as from aggregates with varying *R/S* proportions (Figure 5A). On warming to  $30^\circ\text{C}$ , we obtained *three* distinct lithium resonances, suggesting that **19** may be an ensemble of tetramers (Figure 5B).<sup>27</sup> A Job plot of the relative integration of the three resonances versus the mole fraction of the *R* enantiomer ( $X_R$ ) is illustrated in Figure 6.<sup>28</sup> The curves in Figure 6 correspond to implicit fits of the aggregate populations to the Boltzmann distribution (eqs 5 and 6) for a model based on an ensemble of tetramers.<sup>1,29–31</sup>

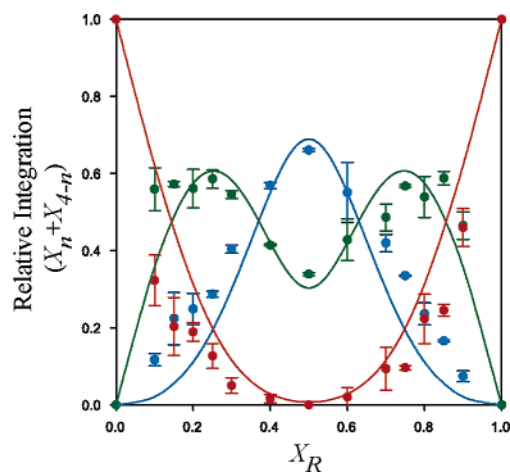


**Figure 6.** Job plot of the mole fraction of  $\text{R}_n\text{S}_{4-n}/\text{R}_{4-n}\text{S}_n$  ( $X_n + X_{4-n}$ ) as a function of the mole fraction of the *R* enantiomer ( $X_R$ ) at  $30^\circ\text{C}$ . The best fit to the data is also shown:  $\text{R}_2\text{S}_2$  (blue);  $\text{R}_1\text{S}_3/\text{R}_3\text{S}_1$  (green);  $\text{R}_4/\text{S}_4$  (red).<sup>32a</sup>

Although some of the qualitative features of the data are reflected in the curves, there are a number of egregious quantitative discrepancies, including a failure to account for the positions of the maxima of the  $\text{R}_3\text{S}_1/\text{R}_1\text{S}_3$  curve and a poor fit to the curvature for each aggregate.

$$X_R = \frac{\sum_{n=0}^N n \times [\text{R}_n\text{S}_{N-n}]}{\sum_{n=0}^N N \times [\text{R}_n\text{S}_{N-n}]} \quad X_n = \frac{[\text{R}_n\text{S}_{N-n}]}{\sum_{j=0}^N [\text{R}_j\text{S}_{N-j}]} \quad (5)$$

$$[\text{R}_n\text{S}_{N-n}] = C \times \frac{N!}{n!(N-n)!} \times \phi_n \times \exp\left(\frac{n\mu_R + (N-n)\mu_S}{kT}\right) \quad (6)$$

$$\text{where } \phi_n = \phi_{N-n} = \left\langle \exp\left(\frac{-g_P}{kT}\right) \right\rangle$$

Accordingly, we considered the alternative possibility that a fourth resonance, characteristic of an ensemble of *hexamers*, was failing to resolve. From distortions in the fit to the tetramer model, we suspected that the fourth resonance, corresponding to  $\text{R}_2\text{S}_4/\text{R}_4\text{S}_2$ , might be concealed by the resonance of  $\text{R}_3\text{S}_3$ . Figure 7 shows the least-squares fit to the data, assuming that the three resonances are  $\text{R}_6/\text{S}_6$ ,  $\text{R}_1\text{S}_5/\text{R}_5\text{S}_1$ , and  $\text{R}_2\text{S}_4/\text{R}_4\text{S}_2/\text{R}_3\text{S}_3$ . The fit to the hexamer model is approximately three times better than the fit to the tetramer model. The free energies for the equilibria described in eqs 7–9 are listed in Table 2. Curiously,

- (26) (a) Arvidsson, P. I.; Ahlberg, P.; Hilmersson, G. *Chem.–Eur. J.* **1999**, *5*, 1348–1354. (b) Bauer, W. *J. Am. Chem. Soc.* **1996**, *118*, 5450–5455. (c) Bauer, W.; Griesinger, C. *J. Am. Chem. Soc.* **1993**, *115*, 10871–10882. (d) DeLong, G. T.; Pannell, D. K.; Clarke, M. T.; Thomas, R. D. *J. Am. Chem. Soc.* **1993**, *115*, 7013–7014. (e) Thomas, R. D.; Clarke, M. T.; Jensen, R. M.; Young, T. C. *Organometallics* **1986**, *5*, 1851–1857. (f) Bates, T. F.; Clarke, M. T.; Thomas, R. D. *J. Am. Chem. Soc.* **1988**, *110*, 5109–5112. (g) Fraenkel, G.; Hsu, H.; Su, B. M. In *Lithium: Current Applications in Science, Medicine, and Technology*; Bach, R. O., Ed.; Wiley: New York, 1985; pp 273–289. (h) Heinzer, J.; Oth, J. F. M.; Seebach, D. *Helv. Chim. Acta* **1985**, *68*, 1848–1862. (i) Fraenkel, G.; Henrichs, M.; Hewitt, J. M.; Su, B. M.; Geckle, M. J. *J. Am. Chem. Soc.* **1980**, *102*, 3345–3350.
- (27) The temperature required to obtain *intra*-aggregate exchange for  $\beta$ -amino carboxamide enolate **4** is markedly higher than that previously needed for  $\beta$ -amino ester enolate hexamers ( $-50^\circ\text{C}$ ).<sup>1</sup>
- (28) (a) Job, P. *Ann. Chim.* **1928**, *9*, 113–203. (b) Gil, V. M. S.; Oliveira, N. C. *J. Chem. Educ.* **1990**, *67*, 473–478.
- (29) Where  $\mu_R$  and  $\mu_S$  are the chemical potentials of *R* and *S*,  $g_P$  corresponds to the free energy of assembly for each permutation, and  $C$  is a constant.
- (30) Widom, B. *Statistical Mechanics: A Concise Introduction for Chemists*; Cambridge University Press: New York, 2002.
- (31) For an example of a Job plot for an ensemble of tetramers, see: Desjardins, S.; Flinois, K.; Oulyadi, H.; Davoust, D.; Giessner-Prettre, C.; Parisel, O.; Maddaluno, J. *Organometallics* **2003**, *22*, 4090–4097. For an early application of a Job plot to assign the stoichiometry of equilibrating species, see: Weingarten, H.; Van Wazer, J. R. *J. Am. Chem. Soc.* **1965**, *87*, 724–730.

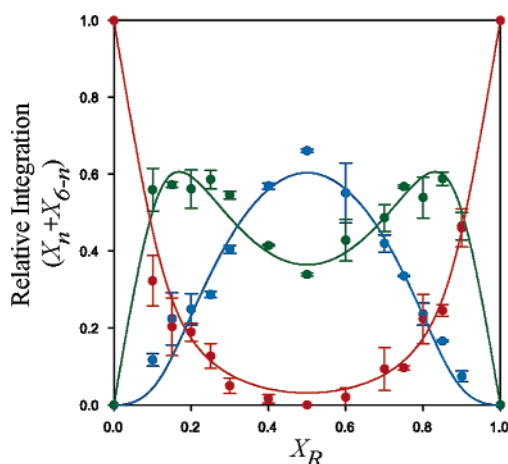


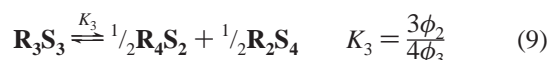
**Figure 7.** Job plot of the mole fraction of  $R_nS_{6-n}/R_{6-n}S_n$  ( $X_n + X_{6-n}$ ) as a function of the mole fraction of the  $R$  enantiomer ( $X_R$ ) at 30 °C. The best fit to the data is also shown:  $R_3S_3/R_2S_4/R_4S_2$  (blue);  $R_1S_5/R_5S_1$  (green);  $R_6/S_6$  (red).<sup>32b</sup>

**Table 2.** Results of the Least-Squares Fits Illustrated in Figure 7

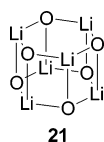
| $K$                     | $\Delta G$ (kcal/mol) <sup>a</sup> |
|-------------------------|------------------------------------|
| $K_1 = 0.046 \pm 0.008$ | $0.0 \pm 0.1$                      |
| $K_2 = 0.52 \pm 0.06$   | $-0.33 \pm 0.07$                   |
| $K_3 = 0.36 \pm 0.08$   | $0.4 \pm 0.1$                      |

<sup>a</sup> The deviations in  $\Delta G$  beyond those expected for a statistical distribution were obtained from the relationship  $\Delta G = -RT \ln(K/K_{\text{statistical}})$ .

if we assume that the  $R_2S_4/R_4S_2$  resonance is obscured by the  $R_1S_5/R_5S_1$  resonance, we obtain a fit of equal quality, yet the resulting free energies indicate that the  $R_2S_4/R_4S_2$  aggregate is absent (Supporting Information).

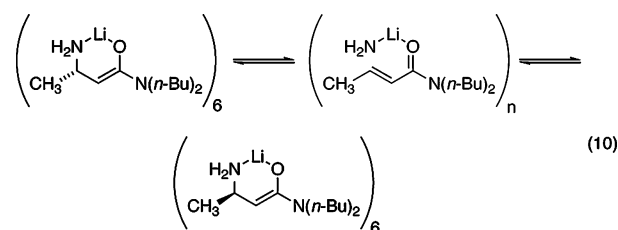


On the basis of analogy to  $\beta$ -amino ester enolates for which a crystal structure was obtained, we tentatively assigned the ensemble of  $\beta$ -amino carboxamide enolates as prismatic hexamers (**21**).<sup>33</sup> Although  $\beta$ -amino carboxamides present steric demands considerably different from those of  $\beta$ -amino esters, it is intriguing that their respective lithium enolates appear to provide isostructural hexamers.

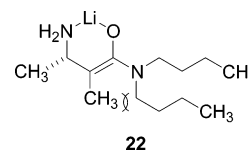


- (32) (a) For the case in which  $n = 2$ , only  $X_2$  is plotted (rather than  $2X_2$ ). (b) For the case in which  $n = 3$ , only  $X_3$  is plotted (rather than  $2X_3$ ).  
 (33) For crystal structures of lithium enolates derived from carboxamides, see: (a) Meyers, A. I.; Seefeld, M. A.; Lefker, B. A.; Blake, J. F.; Williard, P. G. *J. Am. Chem. Soc.* **1998**, *120*, 7429–7438. (b) Bauer, W.; Laube, T.; Seebach, D. *Chem. Ber.* **1985**, *118*, 764–773. (c) Laube, T.; Dunitz, J. D.; Seebach, D. *Helv. Chim. Acta* **1985**, *68*, 1373–1393.

**Racemization.** We noted a curious time-dependent change in the  $^6\text{Li}$  NMR spectra recorded on the enolate homoaggregate. On standing at 30 °C for 2 h, samples of optically pure enolate **4** show  $^6\text{Li}$  resonances indicating racemization. The re-isolated **1** was subjected to  $^1\text{H}$  NMR spectroscopic analysis with the chiral shift reagent (+)-TADDOL,<sup>34</sup> revealing the sample to be 44% ee. While this racemization may add some error in the Job plot data analysis, we obtained reproducible data by acquiring the  $^6\text{Li}$  NMR spectra immediately after removal from a  $-78$  °C bath with a 10 min equilibration at 30 °C. Although the mechanism of the racemization remains unclear, a reversible Michael addition seems possible (eq 10).



**Alkylation.** Under conditions affording <50% conversion to the lithium enolate, treatment with  $\text{CH}_3\text{I}$  (1.2 equiv,  $-78$  °C) affords **2** in high yield (80%) with minimal recovered carboxamide **1**. The high anti selectivity observed is consistent with alkylation at the more accessible face. Kinetic control of the alkylation was evidenced when a 7:1 mixture of **2**:**3** remained unchanged after treatment with excess LiHMDS at  $-78$  °C. The reluctance of **2** and **3** to enolize probably stems from severe allylic strain (**22**).<sup>35</sup>



## Summary

The enolization and alkylation of the unprotected  $\beta$ -amino carboxamide depicted in eq 1 is a deceptively simple reaction. In principle, one could ascertain the overall mechanism for the enolization–alkylation sequence. In practice, however, the reaction is quite complicated owing to a reversible enolization and to the formation of a highly solvent-dependent mixture of mixed dimers, mixed trimers, and homoaggregated enolate hexamers. We also continue to be intrigued by the strategy of determining lithium enolate structures via Job plots.

This study serves as a reminder that optimizing reaction rates, yields, and diastereoselectivities using strategies that are more than simple empiricism continues to pose enormous challenges. In fact, it is fortunate that synthetic chemists convincingly demonstrated the utility of lithium enolates before structural and mechanistic organolithium chemists had the opportunity to reveal the daunting complexity.

- (34) (a) Bussche-Hünnefeld, C.; Beck, A. K.; Lengweiler, U.; Seebach, D. *Helv. Chim. Acta* **1992**, *75*, 438–441. (b) Tanaka, K.; Ootani, M.; Toda, F. *Tetrahedron: Asymmetry* **1992**, *3*, 709–712.  
 (35) (a) Evans, D. A.; Ennis, M. D.; Le, T.; Mandel, N.; Mandel, G. *J. Am. Chem. Soc.* **1984**, *106*, 1154–1156. (b) Hoffmann, R. W. *Chem. Rev.* **1989**, *89*, 1841–1860.

**Acknowledgment.** We thank Gilman E. S. Toombes, Emil Lobkovsky, Ivan Keresztes, and Anthony M. Condo for their analytical support. We also thank the National Institutes of Health and Sanofi-Aventis for direct support of this work. In particular, we would like to thank Timothy A. Ayers, Sithamali V. Chandramouli, and Benoit J. Vanasse of Sanofi-Aventis for enlightening discussions.

**Supporting Information Available:** Experimental preparations, NMR spectroscopic data, IR spectroscopic data (PDF), and X-ray crystallographic data (CIF). This material is available free of charge via the Internet at <http://pubs.acs.org>.

JA043470S